Titration Behavior and Temperature–pH Phase Diagrams for Dilute Aqueous Solutions of Alkenesuccinic Acids and Their Potassium and Sodium Salts

TOYOKO IMAE[1], SACHIKO SUZUKI[1], AKIHITO ABE[1], SHOICHI IKEDA[1],
YOSIO FUKUI[2], MASAMICHI SENOH[2] and KAORU TSUJII[2]

[1]*Department of Chemistry, Faculty of Science, Nagoya University, Nagoya 464 (Japan)*
[2]*Wakayama Research Laboratories, Kao Corporation, Minato, Wakayama 640 (Japan)*

ABSTRACT

The titration curves and the temperature–pH phase diagrams have been drawn for dilute aqueous solutions of alkenesuccinates with alkene groups of C_{12}, C_{14} and C_{16}. The titration curve shifts to higher pH with increasing surfactant concentration or alkene chain length and for potassium salt rather than sodium salt. At lower temperature, the phase diagram shows the wide precipitation region below pH 5.5 and the second precipitation region at higher pH. At higher temperature, opalescence is exhibited between pH 3 and 7, and liquid–liquid phase separation occurs below pH 3. The effects of surfactant concentration, alkene chain length, and counterion species on the phase diagram are discussed.

INTRODUCTION

Alkenesuccinic acid (C_nSA), $CH_3(CH_2)_{n-4}CH{=}CHCH_2CH(COOH)$-$CH_2COOH$, is nonionic at acid pH and changes into ionic form at neutral and alkaline pH. This surfactant shows some characteristic properties in dilute aqueous solutions: C_{12}SA gives viscoelasticity, spinnability and the Weissenberg effect at partially neutralized states [1]. C_{16}SA exhibits iridescent phenomena in the concentration range of 1–2 wt% [2].

In this paper we draw the titration curves and temperature–pH phase diagrams for dilute aqueous solutions of dipotassium and disodium alkenesuccinates (C_nSAK, C_nSANa) and C_nSA at various surfactant concentrations. The effects of alkene chain length, $n = 12$, 14 and 16, and counterion species, K^+ or Na^+, will be discussed.

EXPERIMENTAL

Materials

Samples of $C_{14}SA$, $C_{16}SA$, $C_{12}SAK$, $C_{14}SAK$, $C_{16}SAK$, and $C_{12}SANa$ were prepared in the same way as previously described [1,2]. C_nSA was prepared by hydrolyzing alkenesuccinic anhydride and recrystallizing from acetone. C_nSAK and $C_{12}SANa$ which were obtained by neutralization of C_nSA were precipitated and recrystallized from acetone. The results of gas chromatographic analysis were as follows: $C_{14}SAK$: $C_{14}SAK$, 99.12%, $C_{14}SAK$ (isomer), 0.37%, $C_{16}SAK$, 0.35%; $C_{16}SAK$: $C_{16}SAK$, 98.25%, $C_{16}SAK$ (isomer), 1.01%, $C_{14}SAK$, 0.70%.

Water was redistilled from alkaline potassium permanganate and carbon dioxide gas was removed by boiling for one hour. Standardized solutions of HCl and KOH were purchased from Wako Pure Chemical Inc. Ltd, Osaka.

Preparation of solutions

Aqueous solutions of C_nSAK and $C_{12}SANa$ at surfactant concentrations of $0.02 \sim 0.5 \times 10^{-2}$ g cm^{-3} and of $C_{14}SA$ and $C_{16}SA$ at 0.1×10^{-2} g cm^{-3} were prepared, and an adequate amount of standardized solution of HCl or KOH was added to them in order to adjust pH. After they had been kept overnight at 50°C, pH of each solution was measured. Solutions of $C_{12}SAK$ at surfactant concentrations more than 0.5×10^{-2} g cm^{-3} and of $C_{14}SA$, $C_{16}SA$, $C_{14}SAK$ and $C_{16}SAK$ above 0.1×10^{-2} g cm^{-3} precipitated over a wide pH range. The standardized solution of HCl or KOH was added to solutions by microsyringe in such small amounts that no correction for concentration change was carried out.

Measurements

The pH of solutions was measured on an Iwaki Glass pH/ion meter M-225 under a nitrogen atmosphere, and the degree of ionization, α, was calculated from the difference between the total amount of HCl or KOH added to a solution and the amount of free HCl or KOH, according to the equation

$$\alpha = (C_{H^+,\text{total}} - C_{H^+,\text{free}})/C$$

or

$$\alpha = -(C_{OH^-,\text{total}} - C_{OH^-,\text{free}})/C$$

where C is the molar concentration of surfactant. The pH was determined with an accuracy of ± 0.005.

In order to draw the phase diagram, the solutions were once cooled and precipitated, and then they were kept in a water bath at a desired temperature for
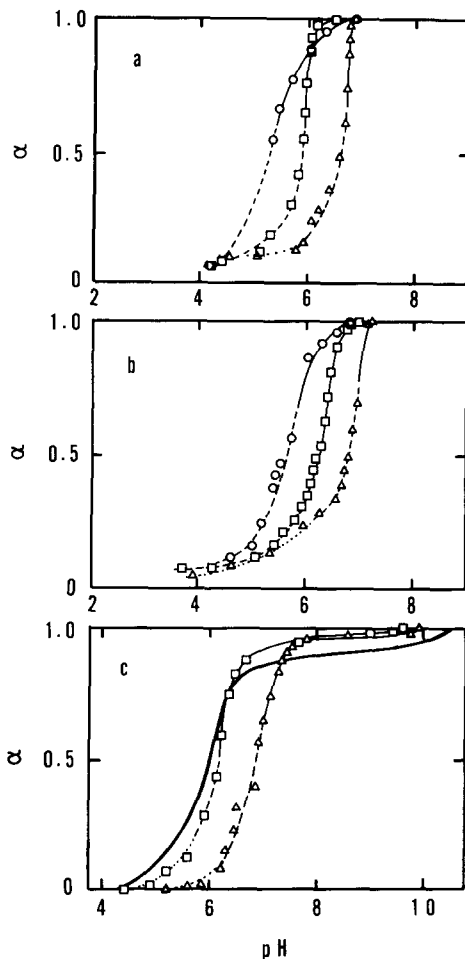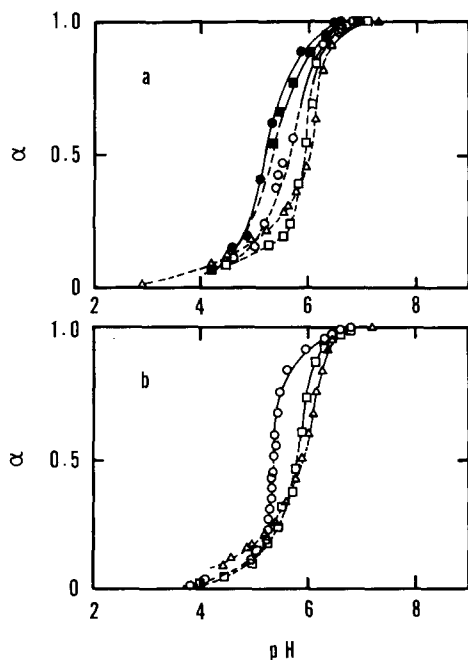
Fig. 1. (left) The titration curves for aqueous solutions of (a) $C_{12}SAK$ and (b) $C_{12}SANa$. Surfactant concentration (10^{-2} g cm^{-3}): ($\bullet$) 0.02; ($\blacksquare$) 0.04; ($\bigcirc$) 0.1; ($\square$) 0.3; ($\triangle$) 0.5. Appearance of solution: (—) clear; (---) opalescent.

Fig. 2. (right) The titration curves for aqueous solutions of C_nSAK and C_nSA. Surfactant and its concentration (10^{-2} g cm^{-3}): (a) C_nSAK, 0.04; (b) C_nSAK, 0.1; (c) C_nSA, 0.1. ($\bigcirc$) $C_{12}SAK$; ($\square$) $C_{14}SAK$ or $C_{14}SA$; ($\triangle$) $C_{16}SAK$ or $C_{16}SA$. Appearance of solution: (—) clear; (---) opalescent; (...) precipitated. The thick solid line drawn in (c) is the titration curve for aqueous solution of $C_{12}SA$ at surfactant concentration of 0.14×10^{-2} g cm^{-3} from Ref. [1].

$3 \sim 4$ hours, within which the phase equilibrium was attained. Temperature was varied from 0 to 75°C.

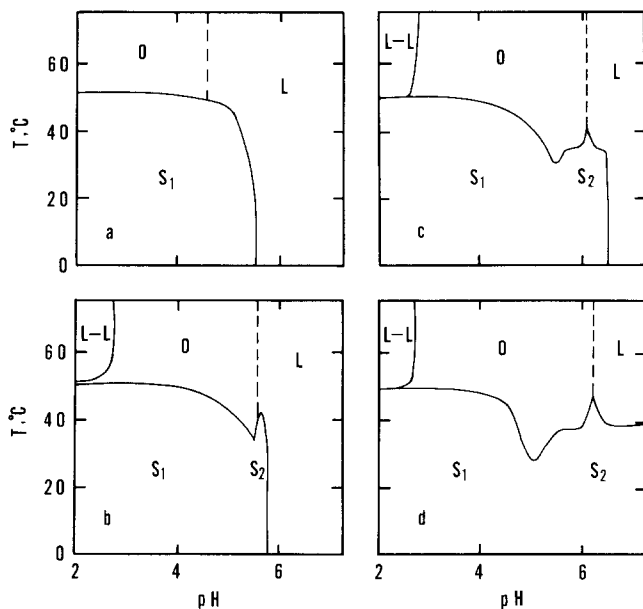The disappearance of precipitation and the occurrence of phase separation and opalescence were visually inspected.

Fig. 3. The phase diagrams for $C_{12}SAK$ in water. Surfactant concentration (10^{-2} g cm^{-3}): (a) 0.04; (b) 0.1; (c) 0.3; (d) 0.5. L, homogeneous region; L–L, two-phase region; O, opalescent region; S, solid region.

RESULTS

Titration

Figure 1 shows the titration curves for aqueous solutions of $C_{12}SAK$ and $C_{12}SANa$ at various surfactant concentrations. While the solutions are clear at neutral pH, they exhibit opalescence at acid pH. As the surfactant concentration is increased, the titration curve generally shifts to higher pH. However, this concentration dependence of the titration curve is reversed at pH lower than 6 for solutions at 0.5×10^{-2} g cm^{-3}, which would be related to stronger opalescence at the higher surfactant concentration. The titration curve of $C_{12}SAK$ shifts to higher pH than that of $C_{12}SANa$.

The titration curves for aqueous solutions of $C_n SAK$ at surfactant concentrations of 0.04 and 0.1×10^{-2} g cm^{-3} are illustrated in Figs 2(a) and 2(b). Solutions of $C_{16}SAK$ separate precipitates at pH below 6. With increasing alkene chain length, the titration curve shifts to higher pH, and opalescence appears at higher pH or at higher degrees of ionization. When the surfactant concentration is increased from 0.04 to 0.1×10^{-2} g cm^{-3}, the titration curve shifts to higher pH and opalescence occurs at higher pH.

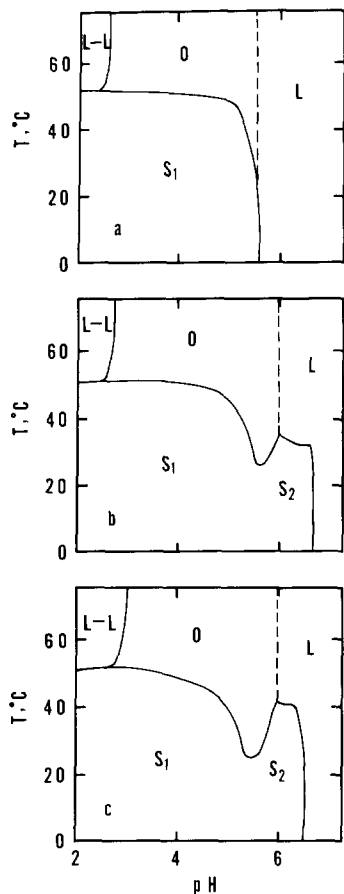The titration curves of $C_{14}SA$ and $C_{16}SA$ at 0.1×10^{-2} g cm^{-3} are given in

Fig. 4. The phase diagrams for $C_{12}SANa$ in water. Surfactant concentration (10^{-2} g cm^{-3}): (a) 0.1; (b) 0.3; (c) 0.5. The signs in figure have same meaning as those in Fig. 3.

Fig. 2(c), which also includes a curve from Ref. [1] for solutions of $C_{12}SA$ at 0.14×10^{-2} g cm^{-3} titrated by NaOH. For α below 0.9, the titration curve changes sharply with an increase in pH, and it shifts to higher pH with increasing alkene chain length. On the other hand, at $\alpha = 0.9 \sim 1$, the titration curve is drifted to higher pH, very differently from that of $C_n SAK$.

Phase diagram

Figure 3 illustrates the phase diagrams for aqueous solutions of $C_{12}SAK$ at various surfactant concentrations. A solution of $C_{12}SAK$ at 0.04×10^{-2} g cm^{-3} gives precipitates at pH lower than 5.5 and at temperatures lower than $52°C$, and a solution at high temperature exhibits opalescence below pH 4.6. For a
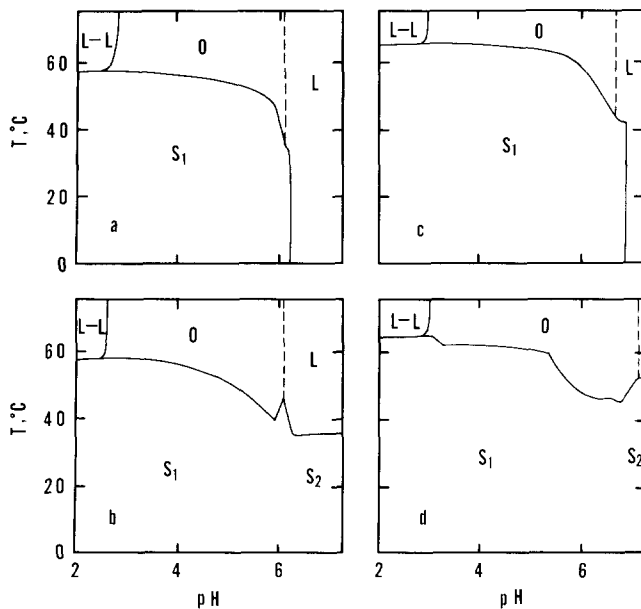
Fig. 5. The phase diagrams for C_nSAK in water. (a,b) $C_{14}SAK$; (c,d) $C_{16}SAK$. Surfactant concentration (10^{-2} g cm^{-3}): (a,c) 0.04; (b,d) 0.1. The signs in figure have same meaning as those in Fig. 3.

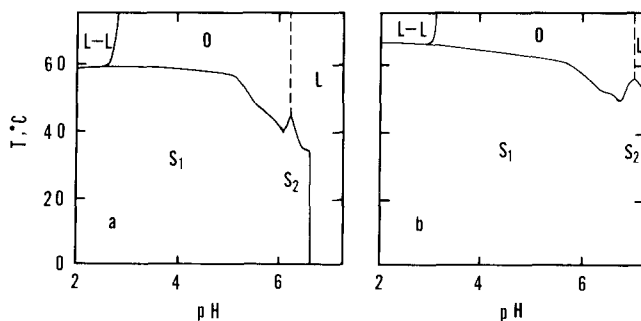Fig. 6. The phase diagrams for C_nSA in water at 0.1×10^{-2} g cm^{-3}. (a) $C_{14}SA$; (b) $C_{16}SA$. The signs in figure have same meaning as those in Fig. 3.

solution at 0.1×10^{-2} g cm^{-3}, while opalescence is observable up to pH 5.6, the liquid–liquid phase separation is manifest below pH 2.8. Moreover, the second precipitation region appears at pH 5.5–5.8. Although one can interpret this region as an extension of the first precipitation region, we have chosen to distinguish them, because the second precipitation region generally has a peak around the limiting pH of the appearance of opalescence. With increasing surfactant concentration, the regions of second precipitation and opalescence extend to higher pH.

Figure 4 indicates the phase diagrams for aqueous solutions of $C_{12}SANa$. The phase diagram and its concentration dependence are very similar to those for $C_{12}SAK$, but the pH region of second precipitation is narrower for $C_{12}SANa$ than for $C_{12}SAK$: the second precipitation arises at pH 5.5–6.5 for $C_{12}SANa$ at 0.5×10^{-2} g cm^{-3}, while its region spreads to pH higher than 7 for $C_{12}SAK$ at the same surfactant concentration.

The phase diagrams for aqueous solutions of $C_{14}SAK$ and $C_{16}SAK$ are given in Fig. 5 and compared with those of $C_{12}SAK$ in Fig. 3. For solutions at 0.04×10^{-2} g cm^{-3}, the precipitation region widens to higher pH and temperature with an increase in alkene chain length, and stronger opalescence arises at higher pH. The liquid–liquid phase separation occurs below pH 3 for $C_{14}SAK$ and $C_{16}SAK$, while it is not observed for $C_{12}SAK$. Although the second precipitation region is not clear for solutions at 0.04×10^{-2} g cm^{-3}, it appears at 0.1×10^{-2} g cm^{-3} and spreads to higher pH with increasing alkene chain length.

The phase diagrams for aqueous solutions of $C_{14}SA$ and $C_{16}SA$ at 0.1×10^{-2} g cm^{-3} are shown in Fig. 6. They are very similar to those of $C_{14}SAK$ and $C_{16}SAK$, except that the pH region of second precipitation is narrower for $C_{14}SA$ than for $C_{14}SAK$.

DISCUSSION

The critical micelle concentration of C_nSA at 45 to 70°C was previously determined by surface tension, solubilization and electric conductivity methods, and it was found to depend on the degree of ionization between $\alpha = 0.7$ and 1.0 and alkene chain length, $n = 12$, 14, or 16 [1]: alkenesuccinate ions formed at neutral pH associate into micelles at higher concentration than nonionic alkenesuccinic acid at acid pH. While the surfactant concentrations of some solutions at α higher than 0.8 in the present work are lower than the critical micelle concentration, solutions at α below 0.8 should have micelles in them.

As seen in Figs 1 and 2, the degree of ionization of alkenesuccinic acid changes sharply at pH 5–7. The titration curve shifts to higher pH with increasing surfactant concentration and alkene chain length and with replacing counterion species, Na$^+$, with K$^+$.

While the pK values of succinic acid are 4.2 and 5.6 [3], alkenesuccinic acid seems to have only one pK value around 5–7. It has reported that the titration curves for nonmicellar solutions of carboxylate soaps had an inflection, but those of micellar soap solutions provided two inflections [4]. Aqueous solutions of lithium and potassium dodecanoates exhibited a transition curve of two steps [5,6], while sodium oleate gave one–step transition [7]. Accompanying the inflection of the titration curve, the occurrence of precipitates [4–6], droplets [3,6,7], or liposomes [3,6] has been reported for solutions of carboxylate soaps.

Being associated with the variation of the titration curve, the temperature–pH phase diagrams of alkenesuccinates in water also change, as shown in Figs 3–6. At pH lower than the inflection of the titration curve where virtually non-ionic alkenesuccinic acid is formed, the precipitation occurs at lower temperature, and opalescence or liquid–liquid phase separation arises at higher temperature, depending on surfactant concentration, although the dependence of liquid–liquid phase separation on surfactant concentration is rather less. Micelles constituted from nonionic surfactant have a lower solubility and tend to coagulate, resulting in precipitation, opalescene, or the formation of oil droplets.

On the other hand, the second precipitation occurs above pH 5.5. Precipitates must be formed by alkenesuccinate salt, since the pH region of the occurrence is higher than the inflection of titration curve. The formation of second precipitation strongly depends on surfactant concentration, being associated with the formation of micelles: alkenesuccinate ions form small ionic micelles, because of electrostatic repulsion between them. When the content of micelles increases over their solubility in water with an increase of surfactant concentration, precipitation occurs.

When counterion species, K^+, is replaced by Na^+, the phase diagram is influenced in such a way that the pH region of second precipitation becomes narrow at higher pH, possibly because of the salting-out effect caused by cationic species.

The effect of alkene chain length on the phase diagram is remarkable: the temperature or pH region of precipitation and opalescence widens and the critical concentration of liquid–liquid phase separation lowers. This behavior must be attributed to the increase in the hydrophobicity of the surfactant.

The solution behavior of surfactants with carboxylate group associated with titration has been discussed by several workers [1,3–9]. Eagland and Franks [8], Lucassen [9], Feinstein and Rosano [4], and Mino et al. [5] indicated the existence of acids, acid–soap complexes, soaps and their aggregates in solutions or precipitates of carboxylate soaps and evaluated their composition from the theoretical analysis of titration curves.

Hargreeves and Deamer [6] and Haines [3] discussed the possibility of the formation of stable acid–soap pairs through unusually strong hydrogen bonding results in the construction of liposomes from single chain carboxylate soaps and their proton-pumping ability. Drzymala [7] considered chemical species in the bulk and on a droplet surface of aqueous droplet dispersions from the titration curves of sodium oleate.

Tsujii et al. [1] reported that dynamic rigidity, surface tension, and specific conductivity of aqueous $C_{12}SA$ solutions are quite unique at pH $5\sim7$ or $\alpha = 0.2 \sim 0.8$. They interpreted this behavior as being the result of the variation in micelle shape, i.e., the formation of rod-like micelles, depending on pH. Similarly to carboxylic acids, alkenesuccinic acid has a structure capable of form-

ing an intermolecular acid–ion hydrogen bond at half neutralization as well as an intramolecular hydrogen bond. Such acid–ion pairs stabilize micelles and then the mixed micelles should become large at this pH region.

Recently, Satoh and Tsujii [2] have found that aqueous solutions of $C_{16}SA$ at a concentration of 1–2 wt% exhibit iridescence, suggesting the formation of lamellar liquid crystal with extremely long spacing distance. Aqueous solutions of alkenesuccinates are opalescent in pH region 3–7, even at low surfactant concentrations of less than 0.5×10^{-2} g cm^{-3}. This suggests that lamellar-like micelles are formed in opalescent solutions.

In conclusion, the variation in micelle shape of alkenesuccinates with a change of pH can be estimated as follows:

(1) At high pH, small ionic micelles are formed and they are generally soluble in water.

(2) When pH is decreased to around $\alpha = 0.5$, large micelles stabilized by acid–ion pairs are formed. They are insoluble in water at room temperature.

(3) At low pH, less than $\alpha = 0.5$, mostly nonionic micelles take a lamellar-like shape and their solutions at high temperatures are opalescent.

(4) Below pH 3, fully nonionic micelles or surfactants have less affinity for water even at high temperatures and solutions separate into solute-rich and poor-liquid phases.

REFERENCES

1 K. Tsujii, N. Saito and T. Takeuchi, J. Colloid Interface Sci., 99 (1984) 553.
2 N. Satoh and K. Tsujii, J. Phys. Chem., 91 (1987) 6629.
3 T.H. Haines, Proc. Natl. Acad. Sci. U.S.A., 80 (1983) 160.
4 M.E. Feinstein and H.L. Rosano, J. Chem. Phys., 73 (1969) 601.
5 J. Mino, E. Matijević and L. Meites, J. Phys. Chem., 80 (1976) 366.
6 W.R. Hargreeves and D.W. Deamer, Biochemistry, 17 (1978) 3759.
7 J. Drzymala, J. Colloid Interface Sci., 107 (1985) 442.
8 D. Eagland and F. Franks, Trans. Faraday Soc., 61 (1965) 2468.
9 J. Lucassen, J. Phys. Chem., 70 (1966) 1824.